THE PROPERTIES OF THE WOOD-POLYSTYRENE INTERPHASE DETERMINED BY INVERSE GAS CHROMATOGRAPHY

John Simonsen
Assistant Professor

Zhenqiu Hong
Graduate Student
Department of Forest Products
Oregon State University
Corvallis, OR 97331

and

Timothy G. Rials
Research Physical Scientist
USDA Forest Service
Southern Experiment Station
Pineville, LA 71360

(Received April 1996)

ABSTRACT

The properties of the interphase in wood-polymer composites are important determinants of the properties of the final composite. This study used inverse gas chromatography (IGC) to measure interphasal properties of composites of polystyrene and two types of wood fiber fillers and an inorganic substrate (CW) with varying amounts of surface coverage of polystyrene. Glass transition temperatures, thermodynamic parameters, and the London component of the surface free energy (Y_s^L) were determined. Values for Y_s^L became constant at higher coverages, allowing the thickness of the interphase to be estimated.

Keywords: Inverse gas chromatography, wood, plastic, polystyrene, interphase, interface, composite.

INTRODUCTION

Wood-plastic composites have been intensively studied in recent years (Woodhams et al. 1984; Takase and Shiraishi 1989; Yam et al. 1990; Maldas and Kokta 1991), particularly the development of composites made from wood and polypropylene (PP), polyethylene (PE), polystyrene (PS), poly(vinyl chloride) (PVC), and polyester (Yam et al. 1990). Wood-plastic composites manufactured from these materials offer many potential benefits, such as low cost, increased stiffness, recyclability, ease of processing, flexible design of properties, and higher strengths than unreinforced plastics. These composites also provide the opportunity to use recycled plastics and recycled wood as raw materials (Rowell et al. 1993).

A fiber-reinforced plastic can be considered to consist of three phases: the bulk plastic matrix, the fiber filler, and the interphase between the two. The strength of the interphase depends on the extent of bonding between the plastic and the filler. That bonding may include mechanical, covalent, ionic, and hydrogen bonds and van der Waals forces. The van der Waals force includes dipole-dipole interactions, induced dipole interactions, and London dispersion forces.

Although many technological advances have improved the material properties of these composites, problems still remain, primarily the lack of adhesion between the wood and the plastic (Kishi et al. 1988). Wood fiber is a hydrophilic material that contains cellulose,

Wood and Fiber Science, 29(1), 1997, pp. 75–84

hemicellulose, lignin, and other extractive compounds. Most plastics, such as PS, PE, and PVC, however, are hydrophobic materials. The different polarities of the fibers and the plastics lead to incompatibility and, therefore, poor bonding in the interphase region between them. This prevents the necessary stress transfer from the plastic matrix to the load-bearing fiber, relegating the function of the fiber to that of a nonreinforcing filler (Hon and Chao 1993). Typically, little of the strength and stiffness of the fiber is translated to the final material properties of the composite when the wood and plastic are poorly bonded. Under stress, the poorly bonded composite will fail when the fibers pull out from the plastic matrix. Thus, the properties of the composite, especially the ultimate properties, are largely determined by the interphase.

The problem of limited adhesion has been extensively addressed in numerous reports on the effects of compatibilizers and coupling agents on the mechanical properties of composites (Woodhams et al. 1984; Maldas et al. 1989; Liang et al. 1994; Sanadi et al. 1994; Youngquist 1995). Although those studies have provided considerable insight into potential solutions, their evaluation of composite performance has been primarily focused on secondary properties rather than on the specific characteristics of the interphasal region within the material system. Therefore, very little understanding has been gained on the fundamental physicochemical parameters that control the structure and properties of the wood fibers/polymer matrix interphase. In this study, we used inverse gas chromatography (IGC) to investigate the interphasal properties of two types of wood-plastic composites.

INVERSE GAS CHROMATOGRAPHY

There are few experimental techniques which yield data that can be mathematically related to the properties of the interphase. One such technique is IGC (Braun and Guillet 1976; Schreiber and Lloyd 1989), which was developed on the basis of conventional gas chromatography (GC) in the late 1970s (Smidsrod and Guillet 1969). The instrumentation of GC and IGC is similar. In IGC, a nonvolatile material to be investigated is packed in a GC column. This stationary phase is then characterized by injecting known volatile chemical compounds, called probes, into the column. The time required for the probe to pass through the column is called the retention time, t_R, which can be translated into a number of important thermodynamic parameters. The obtained thermodynamic data can be related to the properties of the stationary phase (Bolvari et al. 1989).

Retention times can be normalized by injecting a marker, for example methane, which gives a marker retention time, t_m. Net retention volume (V_N) is then calculated from the following equation (Demertzis and Kontomibas 1989):

$$V_N = F\, j\, (t_R - t_m) \qquad (1)$$

where F is a corrected flow rate of the carrier gas and j is a pressure-gradient correction factor for gas compressibility given by (Braun and Guillet 1975; Conder and Young 1979):

$$j = \frac{3}{2}\left[\frac{(P_I/P_o)^2 - 1}{(P_I/P_o)^3 - 1}\right] \qquad (2)$$

where P_i and P_o are the inlet and outlet pressures of the GC column (Braun and Guillet 1975).

At small concentrations of the probe, the retention volume obeys Henry's law at zero coverage (infinite dilution) (Dorris and Gray 1980):

$$V_N = K_S\, A \qquad (3)$$

where K_S = the surface partition coefficient for the adsorbate (m), and A = the total surface area of adsorbent in the column (m^2).

It is normal practice to express V_N as a specific net retention volume at 0°C and per gram of adsorbent;

$$V_g^0 = \frac{273.15}{T_c}\cdot\frac{}{W} V_N \qquad (4)$$

where W = the weight of the adsorbent in the column and T_c = the column temperature.

The retention behavior of probes changes as the temperature rises through T_g (Braun and Guillet 1975, 1976). Below the T_g, the retention time of the probe arises mainly from adsorption of the probe onto the surface of the stationary phase, and $\ln(V_g^0)$ decreases linearly with increasing temperature. When the temperature reaches T_g, probe molecules begin absorption into the PS because of the increased mobility in the PS molecular backbone, resulting in an inflection point on the $\ln(V_g^0)$ vs. 1/T plot. Thus IGC data can be used to determine the T_g in our simulated interphase, which may then be tracked as a function of PS loading, or equivalently, interphase depth.

Gray and coworkers (Mohlin and Gray 1974) extended the IGC technique to the study of fibers. Further development of the theory allowed thermodynamic functions of adsorption to be derived from retention volume data (Kamden and Reidl 1991):

$$\Delta G_A^0 = -RT \ln\left(K_s \frac{P_{s,g}}{\cap_s}\right) \tag{5}$$

$$\Delta H_A^0 = -R \frac{d(\ln V_g^0)}{d\left(\frac{1}{T}\right)} \tag{6}$$

$$\Delta S_A^0 = -\frac{(q_d + \Delta G_A^0)}{T} \tag{7}$$

where q_d = the differential heat of adsorption of the injected probe (kJ/mol); at zero coverage, $q_d = \Delta H_A^0$; T = column temperature (K); $P_{s,g}$ = adsorbate vapor pressure at the standard state; $\cap_s$ = the reference two-dimensional surface pressure, defined by De Boer (Dorris and Gray 1981).

In the case of a nonpolar liquid adhered to a solid surface, the work of adhesion can be separated into two terms (Kamden and Reidl 1991):

$$W_A = 2(\gamma\, \gamma_S^L)^{1/2} \tag{8}$$

where γ = the surface tension of the nonpolar liquid, and γ_S^L = the London component of the solid surface free energy.

Dorris and Gray (1980) used this concept for an homologous series of alkanes. They assumed W_A to be equal to the free energy of adsorption per unit area of the surface, or

$$W_A = -\frac{\Delta G_A^0(CH_2)}{N\, a_{CH_2}} \tag{9}$$

where N = Avogadro's number and a_{CH2} = the surface area occupied by an incremental CH_2 group on an alkane. $\Delta G^0_A(CH_2)$, the surface free energy of adsorption of an incremental methylene group, is obtained by measurement of the free energy of adsorption at infinite dilution for an homologous series of alkanes. Thus the value for the surface free energy may be obtained from IGC data.

Using a value of 0.06 nm^2 for a_{CH2}, and the known value for the surface tension of a methylene unit, the London component of the surface free energy may be calculated from:

$$\gamma_s^L = \frac{1}{4}\frac{1}{\gamma_{CH_2}}\left(\frac{\Delta G_A^0(CH_2)}{N\, a_{CH_2}}\right)^2 \tag{10}$$

Kamdem and Riedl (1991) used this technique to study the surface of chemithermomechanical pulp (CTMP) fiber onto which methyl methacrylate (MMA) had been grafted through the xanthate procedure of Maldas et al. (1989).

Garnier and Glasser (data presented at the ACS National Meeting, August 1992) demonstrated that IGC may be useful for characterizing the surface of model cellulosic beads that were modified by grafting. Determining the acid-base components of the surface energy allowed the estimation of an adhesion parameter for various combinations of polymer matrix and modified filler. From that approach, combined with dynamic mechanical analysis, they were able to identify an interphasal layer of immobilized polymer chains and relate its influence to composite properties.

Inverse gas chromatography has been useful in characterizing the surface of modified lignocellulosic material as it affects adhesion to thermoplastic polymer matrices. In our study, IGC was used to monitor the development and structure of the interphase region by charac-

Aldrich Chemical Company, Milwaukee, Wisconsin, and were used without further purification.

Sample surface areas were measured with N_2 BET adsorption (Table 1). Due to limited resources and equipment difficulties, only a limited number of samples were measured.

ESCA surface analysis

Selected samples were analyzed with a Surface Science model SSX-100 ESCA spectrometer. An aluminum X-ray anode was used with a quartz monochromator and a 600μ spot size. Charge neutralization was conducted on all samples with an electron flood gun and an Ni screen stabilized at ground potential 0.5 mm above each sample. Results were plotted as total oxygen to total carbon (O/C_{total}) and, additionally for CW, total silicon to total carbon (Si/C_{total}).

RESULTS AND DISCUSSION

Inverse gas chromatography

The retention times of the probes were obtained directly from IGC chromatograms. The coefficient of variability was typically less than 3%.

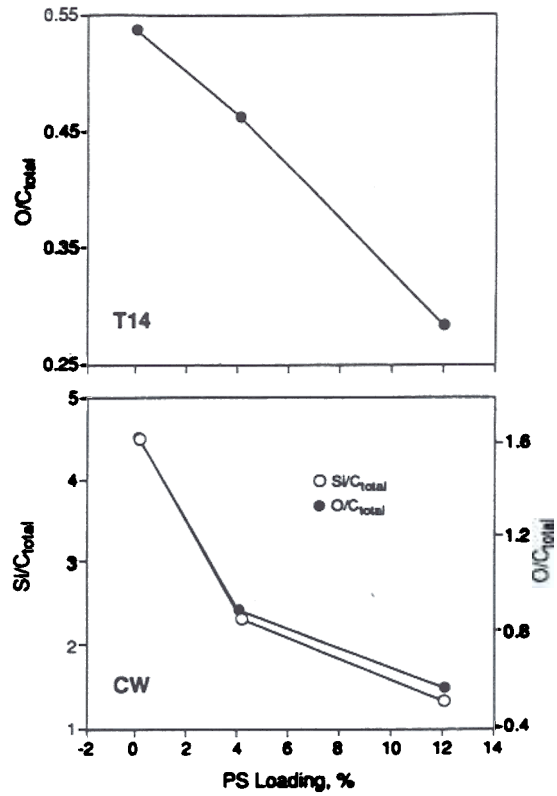

FIG. 1. Silicon/carbon$_{total}$ and oxygen/carbon$_{total}$ from ESCA scans of CW and T14 columns.

ESCA analysis

The ESCA scans of the samples show the progressive PS coverage of the CW and T14 columns (Fig. 1). In the CW column, the Si/C_{total} and O/C_{total} ratios appeared to show some leveling off from 4 to 12% PS loading. The T14, however, showed an approximately linear decrease in O/C_{total} with increased PS loading, suggesting that coverage may not be complete even at 12% PS loading. The IGC results presented below support these observations.

Glass transition temperatures

The T_g for PS* coated on TMP was determined with n-decane (Fig. 2). In the temperature range from 50°C to 70°C, below the PS* T_g, plots of $\ln(V_g^0)$ vs. $1000/T$ were linear. Linear regressions of these values were used to form baselines for each PS* loading. The measurement of T_g required determining the in-

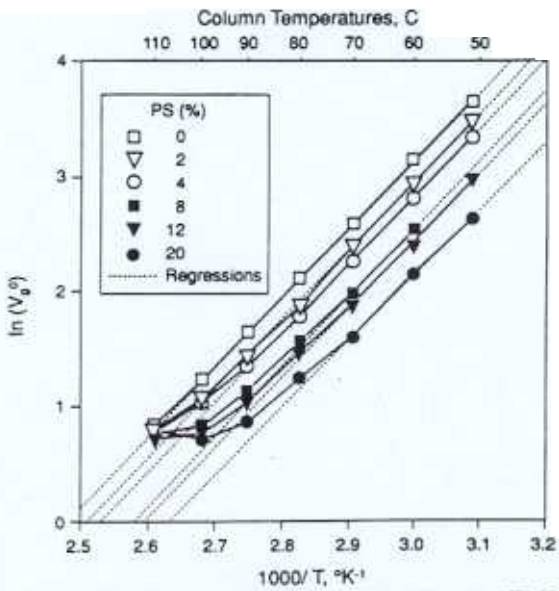

FIG. 2. Glass transition temperatures for PS*-coated TMP from plots of $\ln(V_g)$ vs. $1000/T$.

TABLE 3. *Estimated T_g from IGC.*

Column	
TMP-2%PS*	85–95
TMP-4%PS*	85–95
TMP-8%PS*	65–75
TMP-12%PS*	65–75
TMP-20%PS*	65–75

tersection of the plotted data line and the regression (Table 3). The T_g transition observed here was broader than that observed on other substrates (Lipatov and Nestorov 1975). This may be due to the variability of the wood solid phase, which resulted in a variety of PS* morphologies on the surface with a correspondingly broad distribution of T_g's. While this broad transition did not allow for precise comparisons between different PS* loadings, the T_g appeared to be >80°C for 2 and 4% PS* loading and ~70°C for 8, 12, and 20% loadings. On other substrates, T_g has appeared higher at low surface loadings (Lipatov 1967). This is presumably caused by the restricted mobility of the initially adsorbed polymer layers. As the thickness of the adsorbed polymer layer increases, surface effects should diminish, and the T_g would be expected to approach that of the bulk matrix. The 10°C temperature interval for determination of T_g limited the accuracy of the measurement.

Values for thermodynamic parameters

Enthalpies were obtained from Van't Hoff plots (Eq. 6) for 0% PS-CW and 12% PS-T14. Enthalpies of adsorption, which include the enthalpy of vaporization of the probe at 60°C, were derived for CW, T14, and TMP from the linear regressions of plots of $\ln(V_g^0)$ vs. 1000/T using Eq. (6) for the temperature range 50° to 70°C (Fig. 3). The enthalpies for CW decreased from 0 to 4% PS loading and then became relatively constant. This may have been caused by the increasing coverage of the substrate surface by the PS. If the only surface available to the probe is PS, the enthalpy should be constant. Further additions of PS will add to the depth of the PS layer on the CW, but will not alter the enthalpy.

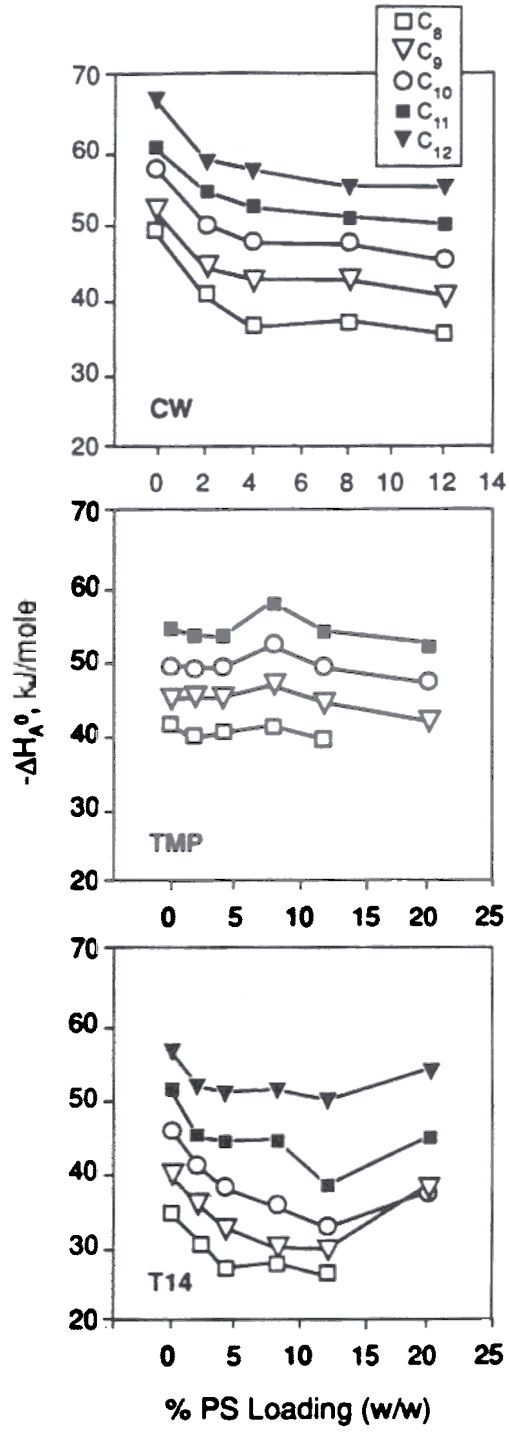

FIG. 3. Enthalpy of probe adsorption on CW, TMP, and T14 substrates as a function of PS loading.

TABLE 4. *Comparison of enthalpy values for CW and TMP.*

Probe	$-\Delta H_A^0$, kJ/mole		Difference (%)
	12%PS-CW	20%PS*-TMP	
C_9	35.3	39.2	11
C_{10}	40.6	41.9	3.2
C_{11}	45.2	47.5	5.1
C_{12}	50.2	52.6	4.8

The results for the wood solid phases were more variable: the TMP results showed a maximum and the T14 showed a minimum enthalpy. The reasons for this are unclear, but may reflect the formation of energy sites different from either the uncoated wood substrate or the bulk matrix PS (or PS* for TMP) phase. Another possibility is that adsorption was not the only interaction between the probe and the solid phase. If the probes were being absorbed to some extent, and that adsorption was a function of probe size, then we would expect to see irregular results. Even so, comparison with the monotonically decreasing shape of the CW graph suggests that there was some interaction, as determined by enthalpy measurements, between the wood substrate and the PS that changed the behavior of the probes.

The enthalpies of the CW and TMP columns tended toward the same value at higher (12 and 20%, respectively) PS loadings (Table 4). We would expect the enthalpy to become constant at higher loadings because the solid phase should be completely covered with PS; therefore, the probe would be interacting only with PS (or PS*). The enthalpy of the T14 column did not level off with increasing PS loading, as did the CW and TMP columns. Since the surface areas were similar (see Table 1), we expected the depth of the PS layer to be similar also. There are several possible explanations for this behavior, such as absorption of the probe into the PS, migration of Douglas-fir extractives from the T14 into the PS, or PS-T14 interactions that gave rise to an altered PS morphology on the surface. Additional research is required to explain this behavior.

Both of the wood solid phase columns appeared to show more variability in the values

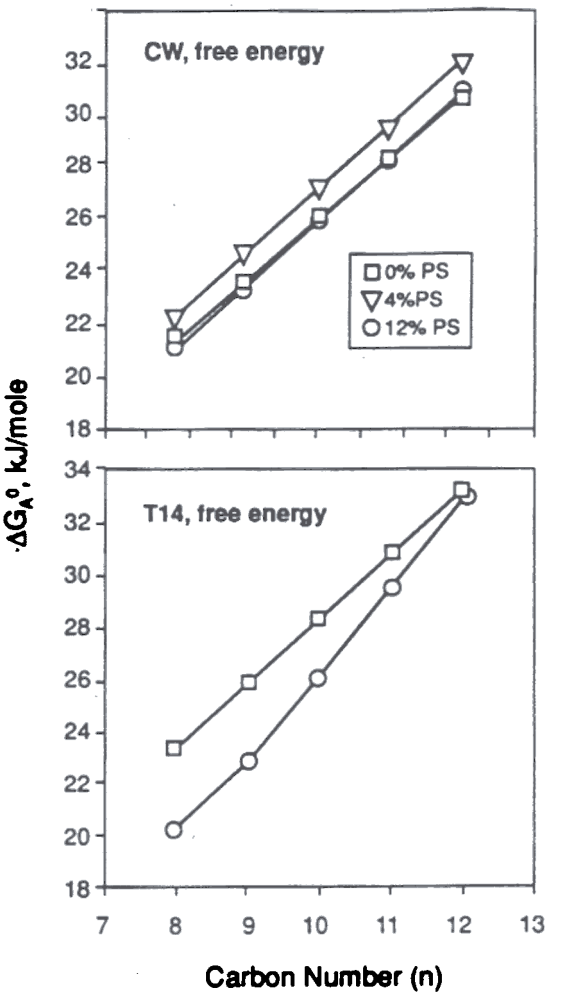

FIG. 4. Free energy as a function of probe carbon number for PS-coated CW and T14 substrates.

of the measured thermodynamic parameters than did the CW column, probably reflecting the greater variability of the wood substrate. The free energy of adsorption was calculated from the retention volume via Eq. (5). Limited data were available because this function requires a value for the surface area. The coated and uncoated CW columns showed decreasing free energy with increasing carbon number (n) (Fig. 4); the values seemed to be independent of the PS loading. The T14 columns also showed decreasing ΔG_A^0 values with increasing n. The PS-coated T14 showed a greater

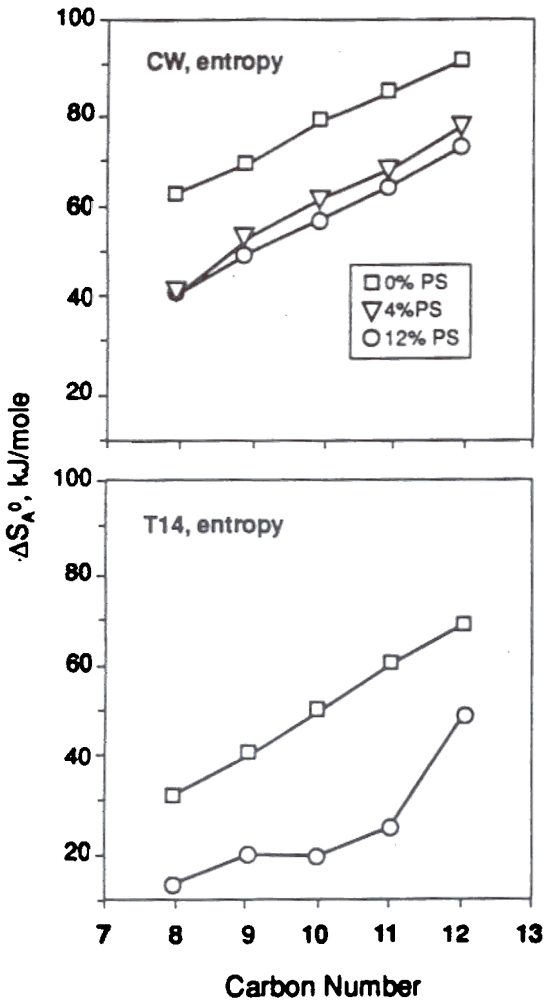

FIG. 5. Entropy as a function of probe carbon number for PS-coated CW and T14 substrates.

slope than the uncoated column, reflecting the differences in adsorption energy for the two different surfaces.

Entropy values were calculated from free energy and enthalpy values via Eq. (7) (Fig. 5). The coated and uncoated CW columns showed similar slopes of entropy vs. carbon number, with the PS-coated columns showing less negative entropy values. Reflecting the enthalpy results, the CW columns appeared to present only a PS surface to the probes at PS loadings greater than 4%. The 12% PS-T14 column, however, showed a more varied response than

TABLE 5 *Depth of the interphase.*

Substrate	Selected PS loading for interphase depth (β), %	Surface area, m^2/g	Interphase depth, μ
CW	8	0.711	0.12
T14	>20	1.026	>0.23
TMP	12	1*	0.13

did the uncoated column with respect to carbon number. At this point, we lack sufficient data to draw any conclusions about the cause of the nonlinearity in the entropy-carbon number relationship of the 12% PS-T14.

The slope of plots of ΔG_A^0 vs. n yielded the free energy of adsorption of a single methylene unit ($\Delta G^0_A(CH_2)$). That free energy may be converted to the London component of the surface free energy, γ_S^L, via Eq. (10). This parameter was compared among different substrates as a measure of their surface energy (Fig. 6). For the CW columns, γ_S^L rose initially, then leveled off after about 8% PS loading, indicating that, from the perspective of surface energy, additional increments of PS beyond 8% added to the bulk matrix phase and interactions with the CW substrate decreased. The TMP showed different behavior, as γ_S^L decreased with increased PS* loading, then leveled off at about 12% PS*. The final γ_S^L values for CW and TMP were similar, again indicating that the PS coating was not influenced by the underlying surface at higher loadings. γ_S^L for T14 showed very different behavior from that of either CW or TMP; γ_S^L increased to 12% PS loading, then decreased at 20%. Leveling of the curve was not observed, indicating that the T14 surface continued to affect the PS coating even at the higher loadings.

Depth of the interphase

The depth of the interphase was estimated by selecting the PS loading that defined the extent of the interphase (β), assuming that the PS density in the interphase was the same as the bulk density of 1.04 g/cc, and modeling the surface as a flat sheet. If the surface is as-

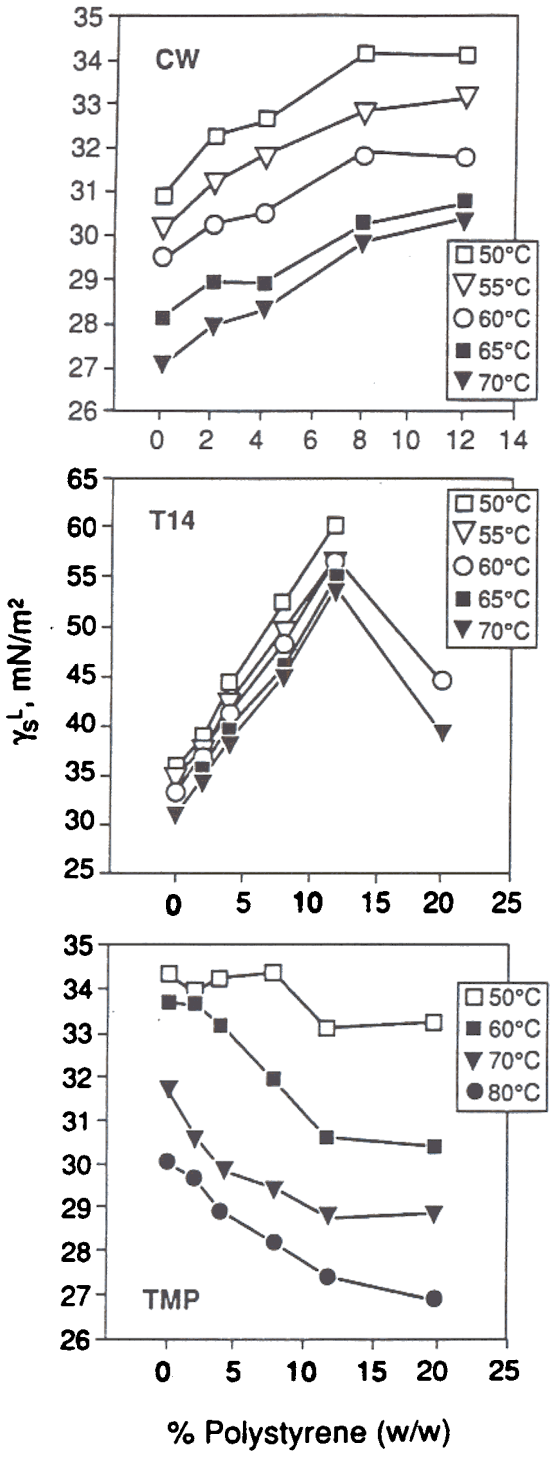

FIG. 6. London component of the surface free energy for CW, T14, and TMP substrates as a function of PS loading.

sumed to be approximated by a flat sheet of the same area as the measured surface area, then the thickness of the interphase will be the volume of the interphase divided by the surface area (Table 5).

$$\text{depth} = \frac{\text{interphase volume}}{\text{surface area}} = \frac{\beta}{\text{surface area} * \text{density}} \quad (11)$$

The interphase depth appeared to be similar for CW and TMP, but noticeably larger for T14. Although our artificially prepared sequences of surfaces may not accurately reflect reality in filled polystyrene composites, they do provide an approximation of the interphase depth. These data support a model of polymer deposition on a substrate surface of constrained polymer backbones in the initial layers, with a gradual transition to bulk polymer backbone morphologies. In this study, the T14 appeared to promote longer range interactions than did either the CW or the TMP.

CONCLUSIONS

The T_g for PS on the various substrates was shown to be a function of the PS loading, i.e., the depth of the interphase. The use of IGC allowed the determination of T_g under conditions difficult or impossible to measure with other techniques. Enthalpy values showed a leveling for CW, a maximum for TMP, and a minimum for T14. Entropy values indicated different interactions between PS and CW or T14. On the basis of γ_s^L values, the depth of the interphase was shown to be approximately 0.1μ. This study demonstrates that inverse gas chromatography can be a powerful tool for the study of interphases in filled polymer composites.

ACKNOWLEDGMENTS

This project was supported by U.S. Department of Agriculture grant number 19-94-017. The ESCA analyses were performed by the Bureau of Mines Albany, Oregon, Research Center, whose able assistance is gratefully acknowledged.

REFERENCES

BOLVARI, A. E., T. C. WARD, P. A. KONING, AND D. P. SHEEHY. 1989. Experimental techniques for inverse gas chromatography. Pages 12–19 *in* D. R. Lloyd, T. C. Ward, and H. P. Schreiber, eds. Inverse gas chromatography. ACS Symposium Series No. 391, American Chemical Society, Washington, DC.

BRAUN, J. B., AND J. E. GUILLET. 1975. Studies of polystyrene in the region of the glass transition temperature by inverse gas chromotography. Macromolecules 8(6): 882–888.

———, AND ———. 1976. Study of polymers by inverse gas chromatography. Adv. Polym. Sci. 21:107–145.

CONDER, J. R., AND C. L. YOUNG. 1979. Physicochemical measurement by gas chromatography. John Wiley & Sons, New York, NY.

DEMERTZIS, P. G., AND M. G. KONTOMINAS. 1989. Thermodynamic study of water sorption and water vapor diffusion in poly(vinylidene chloride) copolymers. Pages 77–86 *in* D. R. Lloyd, T. C. Ward, and H. P. Schreiber, eds. Inverse gas chromatography. ACS Symposium Series No. 391, American Chemical Society, Washington, DC.

DORRIS, G. M., AND D. G. GRAY. 1980. Adsorption of n-alkanes at zero surface coverage on celluose paper and wood fibers. J. Colloid Interface Sci. 77(2):353–362.

———, AND ———. 1981. Adsorption of hydrocarbons on silica-supported water surfaces. J. Phys. Chem. 85: 3628.

HON, D. N.-S., AND W. Y. CHAO. 1993. Composites from benzylated wood and polystyrenes: Their processability and viscoelastic properties. J. Appl. Polym. Sci. 50:7–11.

KAMDEN, D. P., AND B. REIDL. 1991. IGC characterization of PMMA grafted onto CTMP fiber. J. Wood Chem. Technol. 11(1):57–91.

KISHI, H., M. YOSHIOKA, A. YAMANOI, AND N. SHIRAISHI. 1988. Composites of wood and polypropylenes I. Mokuzai Gakkaishi 34(2):133–139.

LIANG, B-H., MOTT, S. M. SHALER, AND G. T. CANEBA. 1994. Properties of transfer-molded wood-fiber/polystyrene composites. Wood Fiber Sci. 26(3):382–389.

LIPATOV, YU. S. 1967. Physical chemistry of filled polymers. International Polymer Science and Technology Monograph #2, Rubber and Plastics Research Association of Great Britain, Boston Spa, Wetherby, West Yorks, England.

———, AND A. E. NESTEROV. 1975. The influence of thickness of polymeric stationary phase on its properties determined by gas chromatography. Macromolecules 8(6):889–894.

MALDAS, L., AND B. V. KOKTA. 1991. Influence of maleic anhydride as a coupling agent on the performance of wood fiber-polystyrene composites. Polym. Eng. Sci. 31(18):1351–1357.

———, ———, AND C. DANEAULT. 1989. Influence of coupling agents and treatments on the mechanical properties of cellulose fiber-polystyrene composites. J. Appl. Polym. Sci. 37:751–775.

MOHLIN, U-B., AND D. G. GRAY. 1974. Gas chromatography on polymer surfaces: adsorption on cellulose. J. Colloid Interface Sci. 47(3):747–754.

ROWELL, R. M., H. SPELTER, R. A. AROLA, P. DAVIS, T. FRIBERG, R. W. HEMINGWAY, T. RIALS, D. LUNEKE, R. NARAYAN, J. SIMONSEN, AND D. WHITE. 1993. Opportunities for composites from recycled wastewood-based resources: A problem analysis and research plan. Forest Prod. J. 43(1):55–63.

SANADI, A. R., R. A. YOUNG, C. CLEMONS, AND R. M. ROWELL. 1994. Recycled newspaper fibers as reinforcing fillers in thermoplastics: Part I—Analysis of tensile and impact properties in polypropylene. J. Reinf. Plastics Compos. 13:54–67.

SCHREIBER, H. P., AND D. R. LLOYD. 1989. Overview of inverse gas chromatography. Pages 1–10 *in* D. R. Lloyd, T. C. Ward, and H. P. Schreiber, eds. Inverse gas chromatography. ACS Symposium Series No. 391, American Chemical Society, Washington, DC.

SMIDSROD, O., AND J. E. GUILLET. 1969. Study of polymer-solute interactions by gas chromatography. Macromolecules 2:272–275.

TAKASE, S., AND N. SHIRAISHI. 1989. Studies on composites from wood and polypropylene, II. J. Appl. Polym. Sci. 37:645–659.

WOODHAMS, R. T., G. THOMAS, AND D. K. RODGERS. 1984. Wood fibers as reinforcing fillers for polyolefins. Polym. Eng. Sci. 24(15):1166–1171.

YAM, K., B. GOGOI, C. LAI, AND S. SELKE. 1990. Composites from compounding wood fibers with recycled high density polyethylene. Polym. Eng. Sci. 30(11):693–699.

YOUNGQUIST, J. A. 1995. The marriage of wood and nonwood materials. Forest Prod. J. 45(10):25–30.